HHS Public Access

Author manuscript

Neuron. Author manuscript; available in PMC 2017 July 28.

Published in final edited form as:

Neuron. 2016 May 18; 90(4): 795–809. doi:10.1016/j.neuron.2016.03.034.

Cannabinoid Type 2 Receptors Mediate a Cell Type-Specific Plasticity in the Hippocampus

A. Vanessa Stempel[1,9,*], **Alexander Stumpf**[1], **Hai-Ying Zhang**[2], **Tuğba Özdoğan**[1], **Ulrike Pannasch**[1], **Anne-Kathrin Theis**[1], **David-Marian Otte**[3], **Alexandra Wojtalla**[3], **Ildikó Rácz**[3], **Alexey Ponomarenko**[4,5], **Zheng-Xiong Xi**[2], **Andreas Zimmer**[3], and **Dietmar Schmitz**[1,4,6,7,8,*]

[1]Neuroscience Research Center (NWFZ), 10117 Berlin, Germany

[2]Intramural Research Program, National Institute on Drug Abuse, Baltimore, MD 21224, USA

[3]Institute of Molecular Psychiatry, University of Bonn, 53127 Bonn, Germany

[4]NeuroCure Cluster of Excellence, 10117 Berlin, Germany

[5]Leibniz-Institut für Molekulare Pharmakologie (FMP), 13125 Berlin, Germany

[6]Bernstein Center for Computational Neuroscience (BCCN), 10115 Berlin, Germany

[7]Center for Neurodegenerative Diseases (DZNE), 10117 Berlin, Germany

[8]Einstein Center for Neurosciences, 10117 Berlin, Germany

SUMMARY

Endocannabinoids (eCBs) exert major control over neuronal activity by activating cannabinoid receptors (CBRs). The functionality of the eCB system is primarily ascribed to the well-documented retrograde activation of presynaptic CB_1Rs. We find that action potential-driven eCB release leads to a long-lasting membrane potential hyperpolarization in hippocampal principal cells that is independent of CB_1Rs. The hyperpolarization, which is specific to CA3 and CA2 pyramidal cells (PCs), depends on the activation of neuronal CB_2Rs, as shown by a combined pharmacogenetic and immunohistochemical approach. Upon activation, they modulate the activity of the sodium-bicarbonate co-transporter, leading to a hyperpolarization of the neuron. CB_2R activation occurred in a purely self-regulatory manner, robustly altered the input/output function of CA3 PCs, and modulated gamma oscillations in vivo. To conclude, we describe a cell type-specific plasticity mechanism in the hippocampus that provides evidence for the neuronal expression of CB_2Rs and emphasizes their importance in basic neuronal transmission.

[*]Correspondence: vstempel@mrc-lmb.cam.ac.uk (A.V.S.), dietmar.schmitz@charite.de (D.S.).

[9]Present address: Medical Research Council (MRC) Laboratory of Molecular Biology, Cambridge CB2 0QH, UK

SUPPLEMENTAL INFORMATION

Supplemental Information includes Supplemental Experimental Procedures and nine figures and can be found with this article online at http://dx.doi.org/10.1016/j.neuron.2016.03.034.

AUTHOR CONTRIBUTIONS

The study was conceived and designed by D.S. and A.V.S., who also wrote the paper. A.V.S. performed all in vitro electrophysiological experiments with the help of A.S., U.P., and A.-K.T., and A.V.S. analyzed all experiments. H.-Y.Z. and Z.-X.X. contributed the ISH and FACS data. The in vivo electrophysiology was performed and analyzed by T.Ö. and A.P. A.Z., D.-M.O., A.W., and I.R. generated and provided all KO animals. A.S., H.-Y.Z., T.Ö., U.P., and A.-K.T. contributed equally to this study.

INTRODUCTION

The endocannabinoid (eCB) system is one of the main neuromodulatory systems acting in the CNS and is highly conserved across species (Liu et al., 2009). It predominantly functions by modulating neural excitability through presynaptic inhibition of transmitter release and eCB-dependent forms of short- and long-term plasticity (Brenowitz and Regehr, 2005; Carta et al., 2014; Chevaleyre and Castillo, 2004; Hájos and Freund, 2002; Kim and Alger, 2010; Marsicano et al., 2003; Monory et al., 2006; Stella et al., 1997). The eCB-mediated plasticity mechanisms are found at both excitatory and inhibitory synapses in most brain areas (Kano et al., 2009), and they primarily depend on a Ca^{2+}-dependent postsynaptic release of eCBs and the retrograde activation of presynaptically located CB_1Rs, which are abundantly expressed in most cell types (Katona and Freund, 2012; Katona et al., 1999). The retrograde mode of action has first been described for two prominent forms of eCB-mediated short-term synaptic depression: depolarization-induced suppression of inhibition (DSI) and excitation (DSE, for reviews see Castillo et al., 2012 and Wilson and Nicoll, 2002). Yet, depending on the mode of activation, they mediate long-term forms of eCB-mediated plasticity of transmitter release as well (Chevaleyre and Castillo, 2003; Gerdeman et al., 2002; Robbe et al., 2002).

In stark contrast to the vast amount of literature on CB_1R-mediated phenomena, very little is known about the relevance of CB_2Rs in neuronal signaling. Indeed, until recently the CB_2R was referred to as the peripheral cannabinoid receptor (CBR), reflecting its predominant expression in organs of the immune system (Munro et al., 1993) where it participates in the regulation of immune responses and is responsible for the anti-inflammatory effects of cannabis (Buckley et al., 2000). A major problem of studying CB_2Rs has been their low expression levels in the CNS and the lack of reliable antibodies, which has sparked controversy concerning their localization in the brain (Baek et al., 2013; Marchalant et al., 2014). Yet, the generation of CBR knockout (KO) mice (Buckley et al., 2000; Zimmer et al., 1999) and the production of a diverse array of synthetic cannabinoid agents have advanced and facilitated research on CB_2Rs. Especially behavioral studies have advocated the presence of CB_2Rs in the CNS (Onaivi, 2006; Van Sickle et al., 2005) with properties that extend their neuro-immunological function. Anatomical and electrophysiological studies support this notion and suggest a role of CB_2Rs in neural transmission and excitability (den Boon et al., 2012; Gong et al., 2006; Morgan et al., 2009). In the hippocampus, the presence of CB_2Rs has been suggested (Brusco et al., 2008; Kim and Li, 2015; Li and Kim, 2015), but their physiological role is uncertain. Furthermore, it is not clear whether they are expressed neuronally or mainly in cells of the immune system, such as microglia (Schmöle et al., 2015).

In this paper, we provide in vitro and in vivo evidence that functional CB_2Rs are expressed neuronally in the hippocampus and that they mediate a self-regulatory eCB-mediated plasticity in a distinct subset of hippocampal principal cells via modulation of the sodium/bicarbonate co-transporter (NBC).

RESULTS

Backpropagating Action Potentials Induce a Cell Type-Specific Hyperpolarization in Hippocampal Principal Cells

In response to trains of action potentials (APs), we observed a long-lasting membrane potential (V_m) hyperpolarization in CA3 pyramidal cells (PCs), which outlasted the classic after hyperpolarization (AHP). The hyperpolarization persisted for the duration of the recording (up to 20 min after the induction), was as large as ~10 mV (Figure 1A), and was present in all cells tested when recorded in perforated-patch (pp) configuration, in which the intracellular milieu of the recorded cell remains undisturbed. When repeating the above experiment in whole-cell (wc) configuration, we observed a fraction of unresponsive cells, which might explain why this form of plasticity has not been observed before, and thus a cutoff was introduced to classify cells as reactive and unreactive (Figures S1A and S1B; see Experimental Procedures). We compared different recording parameters and found a significant correlation between the access resistance (R_a) and the degree of hyperpolarization (Figures S1C–S1F). We furthermore performed a subset of wc recordings with a potassium gluconate-based internal solution (instead of methanesulfonate) or with 1 mg/ml biocytin, in both of which we observed a complete abolition of the hyperpolarization (data not shown). Although the reasons for this are unresolved, many studies previously have reported that internal solutions and anions alter and interfere with membrane properties (Eckert et al., 2001; Kaczorowski et al., 2007).

To elucidate whether this hyperpolarization is a mechanism common to all hippocampal principal cell types or displays cell type specificity, we examined CA1 PCs and dentate gyrus granule cells (DG GCs, both recorded in pp configuration), as well as CA2 PCs. In contrast to CA3 PCs that hyperpolarized to similar extents independent of their location within CA3, neither CA1 PCs nor DG GCs hyperpolarized in response to AP trains (Figures 1B and 1C). This induction failure could be the result of a different induction threshold. To test for this, we used a theta-frequency burst protocol, consisting of four times as many APs as the standard protocol (see Experimental Procedures), that is known to trigger eCB-mediated long-term depression (LTD) in these cells (Younts et al., 2013). However, this also failed to induce a long-lasting hyperpolarization in CA1 PCs (Figures S2A–S2C). Contrary to this, morphologically identified CA2 PCs did express this form of cellular plasticity (Figures S2D–S2F).

The Long-Lasting Hyperpolarization Is Dependent on the Release of Endogenous 2-AG and Neuronal Cannabinoid Type 2 Receptors

What could be the underlying mechanism of this self-inhibitory long-term plasticity? eCBs are known to modulate many forms of long-term plasticity in the CNS (Chevaleyre et al., 2006), and high-frequency stimulation (HFS) has been shown to lead to the release of 2-arachidonoylglycerol (2-AG) in hippocampal slices (Stella et al., 1997). To assess whether the activity-dependent release of 2-AG—the most ubiquitous eCB in the CNS that is synthesized and released upon a sufficient rise in intracellular calcium (Sugiura et al., 2002)—mediates the plasticity, we recorded from mice lacking the 2-AG-synthesizing enzyme DAGLα (Jenniches et al., 2015). To confirm the lack of 2-AG synthesis in the DAGLα

KOs, we recorded DSI in DAGL$\alpha^{-/-}$ CA3 PCs since 2-AG is the main eCB involved in both DSI and DSE (Hashimotodani et al., 2008). In contrast to wild-type (WT) controls, DSI was completely abolished in DAGL$\alpha^{-/-}$ CA3 PCs, as measured by the change in amplitude and frequency of spontaneous inhibitory postsynaptic currents (sIPSCs; Figures 2A and 2B). Next we tested whether lack of 2-AG would have an effect on the AP-mediated hyperpolarization and found that it also was absent in these animals (Figures 2C and 2D), thereby establishing that this effect is dependent on AP-driven 2-AG release.

The main CBRs that eCBs act on are CB_1 and CB_2. Previously, it has been reported that CB_1Rs activate G protein-coupled inwardly rectifying potassium (GIRK) channels on subsets of cortical neurons in response to AP trains (Bacci et al., 2004; Marinelli et al., 2009). This phenomenon, termed slow self-inhibtion (SSI), also leads to a long-lasting V_m hyperpolarization. To test whether the same mechanism may underlie the hyperpolarization, we recorded CA3 PCs from $CB_1R^{-/-}$ mice, but we found that the effect was fully intact in these animals (Figure 3A). We then recorded CA3 PCs from $CB_2R^{-/-}$ mice (the other main CBR); surprisingly, the effect was absent in these animals, suggesting that CB_2Rs mediate the long-lasting hyperpolarization (Figure 3B).

Assuming that CB_2Rs mediate the AP-induced hyperpolarization, preincubation of slices with CBR antagonists should abolish the effect in WT and CB_1R KO animals. First, we confirmed that the percentage of reactive cells recorded in wc configuration was comparable between $CB_1R^{-/-}$ and WT CA3 PCs and that the hyperpolarization was absent in CB_2R KOs (Figures S3A and S3B). We then preincubated slices with the mixed cannabinoid inverse agonist AM-251 that, as predicted, blocked the AP-induced hyperpolarization in both WT and CB_1R mutant CA3 PCs (Figures S3C and S3D). It is of note that this result indicates that AM-251 efficiently targets CB_2Rs at concentrations that are commonly considered to be CB_1R specific (2–5 μM). In addition, we preincubated slices from $CB_1R^{-/-}$ mice with the CB_2R-specific inverse agonist SR144528 (SR), which successfully blocked the hyperpolarization in all cells tested (Figures S3C and S3D). These results support the presence of functional CB_2Rs that can be blocked pharmacologically.

It is known that CB_2Rs are expressed in macrophage lineage cells including microglia that have been shown to modulate neuronal transmission (Salter and Beggs, 2014). Furthermore, as of yet, direct evidence for the neuronal expression of CB_2Rs is still negligible, due to the lack of specific antibodies and neuron-specific genetic manipulations. Thus, to verify this unexpected finding and to test for the neuronal expression of CB_2Rs, we generated a neuron-specific CB_2R KO mouse in which the CB_2R-encoding gene *Cnr2* is deleted under a synapsin promoter via the Cre/loxP system (Syn-CB_2R KO; see Experimental Procedures; Figure S4). We found that in these mice the hyperpolarization was equally absent as in the constitutive KO (Figure 3C). Importantly, the hyperpolarization in the $CB_2R^{+/+}$ littermate controls was not different from C57BL/6 WT mice (Mann-Whitney test, $p = 0.67$; Figure 3D). As a general control for the properties of CA3 PCs recorded from the mutant mice used, we compared their basic intrinsic physiological properties, which were not different from C57BL/6 or littermate WT mice (Figure S3E). Thus, any changes observed were unlikely to stem from differences in their basal properties. In summary, these results strongly

suggest that the hyperpolarization depends on the activation of neuronal CB_2Rs and is independent of CB_1R activation (Figures 3E and 3F).

To support this finding, we performed in situ hybridization (ISH) assays for CB_2R mRNA in hippocampi of Syn-CB_2R KO (Figures 4A–4C and S4) and CB_2R KO (Figure S6) mice. Figure 4 shows the RNAscope ISH results, illustrating co-localization of *Cnr2* (green) and *Rbfox3* (a neuronal marker gene that encodes NeuN, red) in the majority of hippocampal neurons in the CA3 region in WT mice, but not in Syn-CB_2R KO mice (Figures 4A–4C). We detected similar amounts of CB_2R mRNA in area CA2, but much lower levels in areas CA1 and DG (Figure S5).

We noted that *Cnr2* was still detectable in hippocampal tissue of Syn-CB_2R KO mice (Figure 4C, lower panels), which may reflect *Cnr2* expression in glial cells. To test this hypothesis, we used fluorescence- activated cell sorting (FACS) to separate hippocampal neuronal cells and glial cells (Figure 4D), and then we used qPCR to measure *Cnr2* expression levels in each cell population. We found that *Cnr2* mainly was expressed in NeuN + cells (neurons) in WT mice, while it was substantially reduced (~70% reduction) in Syn-CB_2R KO mice and completely abolished in CB_2R KO mice (Figure 4E). As expected, we detected CB_2R mRNA also in non-neuronal cells in WT and Syn-CB_2R KO mice, but not in CB_2R KO mice (Figure 4E). Unexpectedly, low levels of *Cnr2* gene were still detectable in NeuN+ cells in Syn-CB_2R KO mice (Figure 4E), which may be related to the impurity of the sorted neurons (e.g., a small fraction of glial cells may contaminate the NeuN+ population). To test this hypothesis, we examined *Rbfox3* and the glial marker genes *Itgam*, *Cspg4*, and *Aldh1L1*, which encode CD11b (a microglial marker), NG-2 (an oligodendrocyte marker), and ALDH1L1 (an astrocyte marker), respectively, in each cell population. We detected a small percentage (~25%) of glial markers in the NeuN+ population (Figure 4G, a). Since glial cells also express *Cnr2* (Figure 4E), this may well explain why low levels of *Cnr2* expression (~30%) are detectable in NeuN+ cells of Syn-CB_2R KO mice. As a control, we analyzed the same samples for CB_1R mRNA expression, which was not different between NeuN+ (and NeuN−) cells of WT, Syn-CB_2R KO, and CB_2R KO mice (Figure 4F). To further confirm this finding, we compared *Cnr2* expression among WT, CB_1R, and CB_2R KO mice with classical ISH in combination with immunostainings. We found a similar degree of co-localization of *Cnr2* with NeuN and vGluT2 (a marker for glutamatergic neurons) in WT and CB_1R KO mice, while *Cnr2* was undetectable in the CB_2R KO mice (Figure S5).

The Activity-Induced Hyperpolarization Can Be Mimicked and Occluded by CBR Agonists

As a further line of evidence supporting the presence of functional CB_2Rs, we tested whether we can mimic the AP-driven hyperpolarization by directly activating CB_2Rs pharmacologically. The mixed CBR agonists 2-AG and WIN,55212-2 (WIN) as well as the CB_2R-specific agonist HU-308 (HU) all strongly hyperpolarized CA3 PCs in WT mice (Figures 5A–5C, 5E, and 5F). To confirm that the drug-induced hyperpolarization was indeed due to CB_2R activation and as a control for the specificity of HU for CB_2Rs at the concentration used, we tested 2-AG and HU in slices of (Syn-)$CB_2R^{-/-}$ mice. Neither of the drugs led to a hyperpolarization in these animals, strongly arguing for a purely CB_2R-

dependent mechanism (Figures 5D–5F). Additionally, late application of AM-251 could reverse the hyperpolarization induced by 2-AG, arguing for the same target receptor (Figure 5G). To substantiate the assumption of a shared CB_2R-dependent mechanism between AP-dependent release of endogenous 2-AG and exogenously applied CBR agonists, we performed occlusion experiments. When the agonist HU was applied before AP trains, and also when these stimuli were applied in the reverse sequence, the maximal CB_2R activation via one process occluded the other, as the respective second stimulus failed to elicit an additional hyperpolarization (Figures 5H and 5I).

The Hyperpolarization Is Mediated by a G Protein- and Sodium-Dependent Modulation of the NBC

As CBRs are G protein-coupled receptors (GPCRs), we confirmed that the hyperpolarization is mediated by a G protein-dependent cascade by performing experiments with 0.5 mM GDPβS, a non-hydrolyzable GDP analog that blocks G protein-coupled activity. The inclusion of GDPβS into the pipette abolished the pharmacologically induced hyperpolarization within the manipulated neuron (Figures 6A and 6B), supporting the idea of a cell-intrinsic, G protein-dependent mechanism.

CBRs, like many other neuronal GPCRs, couple to GIRK channels (Ho et al., 1999; Mackie et al., 1995), which at first glance appear as a likely downstream target of CB_2R activation to mediate the hyperpolarization via an extrusion of potassium from the cell. However, when analyzing the pharmacologically induced hyperpolarization, we observed no change in input resistance concurrent with the hyperpolarization (Figures 6C–6E). As a control for a GPCR-dependent activation of GIRK, we recorded from CA3 PCs and applied 1 μM adenosine that is known to act on adenosine receptors that in turn activate GIRK. As expected for a conductance-based mechanism, we found a significant reduction of the R_{in} that was furthermore reversed by the GIRK antagonist SCH-23390 (Figure S7A). In contrast to this, the acute application of SCH-23390 failed to repolarize the V_m of CA3 PCs after the successful induction of the hyperpolarization by both AP-dependent release of 2-AG and pharmacological CB_2R activation (Figure S7B). We also analyzed the current-voltage relationship with step protocols before and after CB_2R activation (Figure 6E). To conclude, in contrast to cortical SSI, which is mediated by GIRK channels, this set of experiments strongly argues against a conductance-based process and the involvement of GIRK channels in the hyperpolarization.

Next we investigated the involvement of ionic gradients and electrogenic pumps. In a first set of experiments, we blocked the sodium/chloride co-transporter KCC2 (with 10 μM VU0240551), the sodium/potassium/chloride co-transporter NKCC (with 10 μM bumetanide), and the sodium/hydrogen exchanger (with 10 μM cariporide), but we could not antagonize the long-lasting hyperpolarization. Further, we removed either chloride or potassium from the media; however, the effect was still fully intact (data not shown). Finally, replacing sodium with N-Methyl-D-glucamin (NMDG) resulted in a complete abolishment of the agonist-induced hyperpolarization (Figure 6F). Furthermore, preincubation with a specific blocker of the NBC prevented the long-lasting hyperpolarization, both for agonistas well as AP-driven induction (Figures 6F–6J), arguing for the specific involvement of the

NBC. To rule out that mere interference with the V_m, via the change of intra- and extracellular sodium concentrations, occludes the hyperpolarization, we preincubated slices with a blocker for the sodium/potassium pump that is expressed in CA3 PCs and has been shown to hyperpolarize neurons in an activity-dependent manner as well (Gustafsson and Wigström, 1983). Yet, in the presence of 10 μM ouabain, the hyperpolarization was fully intact (in contrast to NBC block and NMDG replacement, summary graphs in Figures 6I and 6J). To conclude, we found that the hyperpolarization is dependent on (1) extracellular sodium and its gradient across the membrane and (2) the activity of the NBC.

Acute Reversal of the Hyperpolarization by CB_2R Inverse Agonists

What is the underlying cause of the long-lasting nature of the hyperpolarization? HFS can increase 2-AG levels for several minutes (Stella et al., 1997), and it has been shown that eCB-mediated LTD of inhibitory inputs can be reversed by applying AM-251 5 min, but not 10 min, after the induction (Chevaleyre and Castillo, 2003). Additionally, it has been suggested previously that antagonists can acutely reverse other forms of long-term plasticity such as mGluR-dependent LTD (Palmer et al., 1997), which is likely to be due to a persistent receptor activation even in an agonist-unbound state (Lodge et al., 2013). To test for these possibilities, we first performed control recordings in WT CA3 PCs for >25 min to confirm the feasibility of pharmacological manipulation during longer recordings (Figures S8A and S8B). In a separate set of experiments, we then acutely applied the CB_2R-specific inverse agonist SR after eliciting the hyperpolarization in CA3 PCs with the AP protocol. We found that late application of SR repolarized the V_m back to its baseline levels in all cells tested (Figures S8C–S8E). Because we applied the drug at different time points (~5–15 min after the induction; Figure S8C) and could reverse the hyperpolarization even 15 min after induction, it is unlikely to still depend on elevated 2-AG levels. Thus, this dataset suggests that constitutive receptor activation may be the mechanism underlying the persistency of this particular form of plasticity. We performed these experiments in $CB_1R^{-/-}$ animals to eliminate possible off-target effects of the pharmacological agent.

Comparison of CB_2R-versus Presynaptic eCB-Mediated Effects

Do CB_2Rs also modulate classic eCB-mediated alterations of presynaptic function and does the hyperpolarization have similar characteristics? First, we tested whether the hyperpolarization depends on synaptic transmission and found that it was intact in block of both excitatory and inhibitory transmissions (Figure 7A). Second, DSI has been shown to be a mechanism that acts in an autocrine and a paracrine manner (Kreitzer et al., 2002; Wilson and Nicoll, 2001 but see Younts et al., 2013). To test if the AP-driven release of 2-AG by one neuron is sufficient to elicit a hyperpolarization in neighboring neurons, we performed dual pp recordings of adjacent CA3 PCs (distance between pipette tips: 11 ± 1.2 μm), and we found no evidence for a detectable spread of the effect between PCs (Figures 7C and 7D). Third, to test whether CB_2R activation could mimic DSI, we recorded evoked IPSCs (eIPSCs) in CA3 PCs and induced DSI by depolarization of the recorded neuron. Conversely, subsequent application of 1 μM HU did not alter the eIPSC amplitude of DSI+ neurons (Figure 7E). Additionally, the reduction of field excitatory postsynaptic potentials (fEPSPs, recorded in CA3) observed upon application of the mixed CBR agonist WIN, which is also ascribed a presynaptic mode of action (Takahashi and Castillo, 2006), could

not be mimicked by HU (Figure 7F). To conclude, the hyperpolarization appears to be a solely self-regulatory cell-intrinsic mechanism that acts complementary to presynaptic CBRs.

Physiological Stimulation and Functional Significance of CB_2Rs

We assessed the functional significance of CB_2R activation both on a single cell and on a network level. In stark contrast to the so far employed artificial fixed-frequency induction protocol, both the frequency and amount of neuronal spiking in vivo were irregular, highly variable, and temporally complex. CA3 PCs in particular are known to spike frequently when recorded in vivo, both as single spikes and in bursts (Tropp Sneider et al., 2006). We thus considered whether physiologically relevant activity patterns are able to induce the hyperpolarization, and we constructed a spike train based on in vivo place field firing patterns of CA3 PCs (see Experimental Procedures). Indeed, we found that this physiological spike train (PST) elicited a hyperpolarization with an average ΔV_m that did not differ from the standard protocol (unpaired t test, $p = 0.42$; Figures 8A–8C).

Next we investigated whether the long-lasting hyperpolarization affects the output of CA3 PCs. We therefore compared the spike probability of synaptically evoked AP firing in CA3 PCs before and after the application of HU. In those cells that hyperpolarized (wc: 5/8 reactive cells), we found a simultaneous, robust reduction in spike probability by >80% (Figures 8D–8F). To test whether this was causally linked to the hyperpolarization induced by the CB_2R agonist, we clamped the cells to their initial baseline V_m with constant current injection at the end of each experiment. As expected, this was sufficient to restore the initial spike probability in all neurons (0.93 ± 0.04, normalized to 1). Conversely, when we manually hyperpolarized the unreactive cells with current injections (baseline V_m: −64.7 ± 0.8 mV, hyperpolarized V_m: −72.5 ± 0.5 mV), we were able to mimic the reduction in spike probability induced by the CB_2R agonist-mediated hyperpolarization (0.1 ± 0.036, normalized to 1). In summary, these experiments indicate that the V_m hyperpolarization following activation of CB_2Rs significantly shifts the rheobase of CA3 PCs and profoundly reduces their input/output function.

Finally, to study the role of CB_2R signaling in network dynamics, we recorded local field potentials (LFPs) in area CA3 of freely behaving mice that were systemically treated with the CB_2R agonist HU or vehicle. LFP oscillations in the slow gamma band (30–85 Hz), generated locally in area CA3 (Csicsvari et al., 2003), and theta (5–10 Hz) oscillations determine hippocampal network synchronization and information processing during exploratory behavior. During baseline recordings and after vehicle administration, the amplitude of gamma oscillations changed as a function of the theta phase; more pronounced variations of gamma amplitude were found during theta cycles of higher amplitude (Figure 8G, upper panel), in agreement with earlier reports (Schomburg et al., 2014; Wulff et al., 2009). In contrast, following the agonist administration, slow gamma modulation was significantly less strongly determined by changes of theta oscillation amplitude in WT mice (Figure 8G, lower panel), but not in Syn-$CB_2R^{-/-}$ mice ($F_{1,10} = 0.3$, $p = 0.59$). The power of theta and gamma oscillations as well as the theta modulation of intermediate (65–120 Hz) gamma oscillations were not affected by the agonist treatment (power: $F_{1,13} = 1.0$, $p = 0.33$

and $F_{1,13} = 1.5$, $p = 0.24$; modulation: Figure 8H). Additional LFP recordings in area CA3 of behaving Syn-$CB_2R^{-/-}$ mice and their WT littermates revealed a reduced power of gamma oscillations in the mutant (Figure S9). Altogether, these results suggest that neuronal CB_2Rs regulate gamma oscillations in area CA3 in vivo.

DISCUSSION

CB_2Rs have been reported to be modulated during a variety of complex neuropsychiatric disorders, including depression, schizophrenia, and autism spectrum disorders, and, due to their non-psychotropic mode of action, they are considered promising therapeutic targets (Onaivi, 2011). Yet, in contrast to the well-established function and localization of CB_1Rs, little is known about their role in basic neurotransmission. By providing a first description of functional, neuronally expressed CB_2Rs in area CA3 of the hippocampus, our findings now reveal, to our knowledge, a novel role for CB_2Rs in the CNS, and they challenge the classic, CB_1R-focused view on eCB function.

In summary, we find that neuronal CB_2Rs mediate a long-lasting, cell-intrinsic hyperpolarization in hippocampal principal neurons of areas CA3 and CA2. The CB_2R-dependent hyperpolarization can be triggered via the release of endogenous 2-AG or by direct pharmacological receptor activation. Because it is long-lasting in its nature and is additionally independent of excitatory and inhibitory synaptic transmission, the hyperpolarization appears to be an intrinsic plasticity process that negatively modulates the excitability of CA3 PCs.

Cell Type-Specific Expression of the CB_2R-Mediated Plasticity

The AP-dependent hyperpolarization can only be induced in CA3 and CA2 PCs, which resemble each other in their electrophysiological properties (Wittner and Miles, 2007), but not in the other two main principal cell populations of the hippocampus, namely CA1 PCs and DG GCs. This may be either due to a lack of CB_2R protein or due to an induction failure. The former is unlikely since we detected low levels of CB_2R mRNA in these cell populations as well. We thus tested the latter hypothesis and found that we can readily induce a hyperpolarization of CA1 PCs by pharmacological activation of CB_2Rs with both HU and WIN (data not shown). In combination with the finding that even strong stimuli that are known to trigger eCB-mediated LTD at this synapse (Younts et al., 2013) failed to elicit a hyperpolarization, these results support the notion that functional CB_2Rs are present in CA1 (and DG) but are not activated by physiological activity. Possible explanations for this induction failure are manifold, including differences in the expression levels and distribution of the CB_2R or other components of the ECS, and highlight the fact that the development of specific CB_2R antibodies (Baek et al., 2013; Marchalant et al., 2014) is crucially important to determining their expression on a (sub-)cellular level.

Neuronal Expression of Functional CB_2Rs in Area CA3

The expression of CB_2Rs in the CNS has been subject to much debate (Onaivi, 2006), with many published studies being unable to detect any CB_2R mRNA or ligand binding in brain preparations or only in microglia (Buckley et al., 2000; Galiègue et al., 1995; Schmöle et al.,

2015). However, behavioral and electrophysiological studies have suggested the functional presence of CB_2Rs (Onaivi, 2006; Van Sickle et al., 2005; Xi et al., 2011; Zhang et al., 2014). Therefore, the following question remains: are CB_2Rs expressed in neurons? To address this question, we generated a novel, neuron-specific CB_2R KO to use in combination with electrophysiological and molecular biology techniques. First, the finding that the CB_2R-mediated hyperpolarization is absent in the neuron-specific CB_2R KO argues for the presence of functional neuronal CB_2Rs at a protein level. Second, by means of ISH (with a fluorescence double-labeling strategy) and FACS/qPCR assays, we are able to demonstrate the expression of CB_2R mRNA in hippocampal glutamatergic neurons and, more specifically, CA3 PCs. Taken together, these data provide strong and direct evidence for the neuronal expression of functional CB_2Rs in the CNS.

What Underlies the Long-Lasting Hyperpolarization Mechanistically?

Surprisingly, the hyperpolarization was not accompanied by a change in membrane resistance, which rules out the involvement of a conductance-based mechanism (unlike cortical SSI, Bacci et al., 2004) and suggests the involvement of an ion pump or co-transporter. CBRs have been shown before to modulate the activity of ion co-transporters, such as the sodium/hydrogen exchanger (Bouaboula et al., 1999). Following this lead, we performed experiments with NMDG-based sodium replacement that hinted toward a sodium-dependent process. Finally, block of the NBC by a specific antagonist abolished both the AP-driven and pharmacologically induced hyperpolarization, suggesting it to be the downstream target of CB_2R activation.

The NBC is a member of the SLC4 solute carrier family and plays an important role in intracellular pH regulation by accumulating intracellular bicarbonate driven by the inwardly directed sodium gradient (for a review see Ruffin et al., 2014). Hippocampal PCs express NBCs (Majumdar et al., 2008) and functional studies indicate a role in pH regulation during neuronal activity (Chesler and Kaila, 1992). To our knowledge, our study provides the first evidence for a functional coupling between cannabinoid signaling and the NBC. Future studies will discover the molecular mechanisms involved in this interaction.

A possible cause for the long-lasting hyperpolarization upon CB_2R activation could be identified based on the observation that the acute application of a CB_2R inverse agonist reversed the AP-triggered hyperpolarization. Given that endogenous 2-AG is broken down rapidly (Sugiura et al., 2002) and other studies estimated the prolonged presence of 2-AG after HFS to be ~5 min (Chevaleyre and Castillo, 2003), it is unlikely that 2-AG remains available to constitutively activate the receptor up to 15 min after induction. Thus, our data suggest that the transient stimulation of CB_2Rs by activity-evoked release of 2-AG may alter their properties, rendering them persistently active in the absence of agonist, similar to observations on mGluRs (Lodge et al., 2013; Young et al., 2013).

Complementary Action of CB_1 and CB_2 Receptors

As mentioned in the Introduction, membrane-derived lipids including eCBs predominantly function through presynaptic inhibition of transmitter release. Only few studies have demonstrated changes in neuronal excitability that depend on cell-intrinsic eCB modulation

(Bacci et al., 2004; den Boon et al., 2012). Thus, the question arises, how might CB_2R activation contribute to the fine-tuned, highly complex eCB neuromodulatory system that controls a single neuron's physiology and excitability from presynaptic transmitter release to spike output?

Our data suggest that, on a cellular level, CB_1Rs and CB_2Rs may provide a non-overlapping functionality with CB_1Rs being expressed mostly presynaptically and CB_2Rs on postsynaptic compartments of hippocampal CA3/2 PCs. A complementary modulation of the auto-associative CA3 network by (1) CB_1Rs that presynaptically modulate chemical transmission and alter synaptic weights of incoming inputs and (2) CB_2Rs that alter the cell's intrinsic properties in response to AP firing provides a powerful mechanism to fine-tune the network's excitability. This seems especially important in areas CA3 and CA2 that are recurrently connected and, thus, particularly susceptible to hyperexcitability and imbalanced network states (Le Duigou et al., 2014; Sloviter, 1991). In line with this, the hypothesis of CB_2Rs providing a functional safety brake is plausible. Furthermore, given the long-lasting nature of the hyperpolarization, one might speculate that, especially during ongoing activity in vivo, CB_2Rs will provide a rather tonic inhibition.

Physiological Relevance of CB_2R Activation in the Hippocampus

The in vivo and in vitro analyses of CB_2R function show that they impact the output of a single CA3PC as well as alter locally generated network oscillations in the behaving animal. We show that PSTs activate CB_2Rs and that their activation reduces the spike probability of CA3 PCs. Our finding, that a change in the V_m strongly affects the input/output transformation of CA3 PCs, supports the idea that intrinsic membrane properties are highly relevant for single-cell excitability and information processing (Kowalski et al., 2015; Lee et al., 2012). The hippocampus exhibits several functionally distinct types of gamma oscillations including locally generated, slow oscillations and intermediate/fast oscillations that originate in the entorhinal cortex and entrain the hippocampus (Colgin et al., 2009; Csicsvari et al., 2003; Schomburg et al., 2014). It is thought that the cross-frequency coupling of hippocampal theta and gamma oscillations, as observed during exploratory behaviors, may serve as a coding scheme for working memory and to provide the basis for simultaneously encoding information at different timescales. In the CA3 area gamma oscillations arise from interactions between PCs and interneurons, rendering gamma synchronization sensitive to changes of excitability of these cell types (Buzsáki and Wang, 2012).

We found that acute application of a CB_2R agonist selectively affects the theta-dependent modulation of gamma oscillations in WT mice, but not Syn-$CB_2R^{-/-}$ mice, and that Syn-$CB_2R^{-/-}$ mice exhibit reduced power of gamma oscillations. In contrast, the effects of eCBs on network oscillations in vivo exerted via CB_1Rs are widespread and affect synchronization across frequency bands (Robbe et al., 2006), suggesting a more specific involvement of CB_2R in spatial coding modes supported by gamma oscillations (Bieri et al., 2014). To summarize, the reduced spike probability of CA3PCs in vitro and the selective disruption of slow gamma oscillations by CB_2 Ractivation strongly suggest that neuronal CB_2Rs are important modulators of local network rhythms. Recent studies have suggested that a lack of

CB_2Rs impairs hippocampal memory function (García-Gutiérrez et al., 2013; Li and Kim, 2016), similar to the effect of CB_1R deficit in adult mice (Bilkei-Gorzo et al., 2005). Further electrophysiological and behavioral analyses of the Syn-CB_2R KO will hopefully help us gain a better understanding of their role in hippocampal information processing both on a single cell and on a network level.

Conclusions

In comparison to the vast literature on CB_1R function in the CNS, the current state of knowledge concerning CB_2Rs is negligible. It is thus crucial to highlight their importance in basic neuronal transmission. Our results provide, to our knowledge, a first in-depth description of neuronal CB_2R expression and their functional relevance in the hippocampus.

EXPERIMENTAL PROCEDURES

Ethical Statement and Animal Handling

Animal husbandry and experimental procedures were performed in accordance with the guidelines of local authorities (Berlin, Germany), the German Animal Welfare Act, and the European Council Directive 86/609/EEC. KO mice were maintained on a C57BL/6 genetic background and generated in the laboratory of A.Z. (Buckley et al., 2000; Jenniches et al., 2015; Zimmer et al., 1999). Neuron-specific, conditional CB_2R KO mice were generated by crossing mice expressing Cre recombinase under the Synapsin I promoter with floxed CB_2R animals.

In Vitro Electrophysiology

Electrophysiological recordings from hippocampal slices were made as described previously (Maier et al., 2011, 2012). The AP trains (inter-stimulus interval: 10 ms, inter-train interval: 20 s) were induced with 2-ms-long, somatic- current injections. Pharmacological agents were bath applied. Sample sizes are given as the number of experiments (n) and of animals (N). Normally distributed datasets were compared with a two-tailed Student’s t test and values are expressed as mean ± SEM. Nonparametric tests were used as indicated and data are presented as median (with 25^{th} and 75^{th} percentiles). Results were considered significant at $p < 0.05$. Given V_m values are not corrected for liquid junction potential. In wc recordings, cells were classified as reactive or nonreactive based on a 2.1-mV cutoff.

In Vivo Electrophysiology

Mice were implanted with arrays of single-tungsten wires in area CA3, and the LFP was recorded while the animals explored freely in an open arena. After 1 hr of baseline recordings, animals were injected with either vehicle (10 mg/kg DMSO) or with HU (10 mg/kg, dissolved in DMSO) and were recorded in the arena for 1 hr more. Phase-amplitude coupling of theta and gamma oscillations was computed as described previously (Wulff et al., 2009). The statistical significance of comparisons was determined by a two-way ANOVA.

Molecular Biology

Standard molecular biology techniques as well as classical ISH, RNAscope ISH, and FACS assays were performed as described previously (Buckley et al., 2000; Li et al., 2015; Liu et al., 2014; Zhang et al., 2014). For the RNA-scope ISH in the Syn-CB_2R KO, the probes Mm-*Cnr2*-O2 and Mm-*Rbfox3*- C2 were designed and provided by Advanced Cell Diagnostics. For FACS, cells were sorted with a PE-labeled (fluorescent) anti-NeuN antibody (1:500; FCMAB317PE, Millipore) and validated the purity of the detected cell populations with qRT-PCR analysis of *Rbfox3* and *Itgam*, *Cspg4*, and *Aldh1l1*.

Supplementary Material

Refer to Web version on PubMed Central for supplementary material.

Acknowledgments

We thank S. Rieckmann and A. Schönherr for technical assistance; G. Buzsáki, K. Diba, and R. Schmidt for sharing their data; C. Böhm and F.W. Johenning for unpublished experiments; and I. Vida, I. Katona, and A. Kulik for their help. Also, we thank J.R. Geiger, U. Heinemann, and members of the D.S. lab for helpful discussions; N. Maier for critical comments on an early version of the manuscript; and D. Evans for proofreading the final version. This work was supported by the NeuroCure and the ImmunoSensation Clusters of Excellence, the BCCN, the DZNE, the Einstein Foundation, and the Deutsche Forschungsgemeinschaft (FOR926, SFB665, SFB958, SPP1665, and GRK1123).

References

Bacci A, Huguenard JR, Prince DA. Long-lasting self-inhibition of neocortical interneurons mediated by endocannabinoids. Nature. 2004; 431:312–316. [PubMed: 15372034]

Baek JH, Darlington CL, Smith PF, Ashton JC. Antibody testing for brain immunohistochemistry: brain immunolabeling for the cannabinoid CB_2 receptor. J Neurosci Methods. 2013; 216:87–95. [PubMed: 23583232]

Bieri KW, Bobbitt KN, Colgin LL. Slow and fast γ rhythms coordinate different spatial coding modes in hippocampal place cells. Neuron. 2014; 82:670–681. [PubMed: 24746420]

Bilkei-Gorzo A, Racz I, Valverde O, Otto M, Michel K, Sastre M, Zimmer A. Early age-related cognitive impairment in mice lacking cannabinoid CB1 receptors. Proc Natl Acad Sci USA. 2005; 102:15670–15675. [PubMed: 16221768]

Bouaboula M, Bianchini L, McKenzie FR, Pouyssegur J, Casellas P. Cannabinoid receptor CB1 activates the Na+/H+ exchanger NHE-1 isoform via Gi-mediated mitogen activated protein kinase signaling transduction pathways. FEBS Lett. 1999; 449:61–65. [PubMed: 10225429]

Brenowitz SD, Regehr WG. Associative short-term synaptic plasticity mediated by endocannabinoids. Neuron. 2005; 45:419–431. [PubMed: 15694328]

Brusco A, Tagliaferro P, Saez T, Onaivi ES. Postsynaptic localization of CB2 cannabinoid receptors in the rat hippocampus. Synapse. 2008; 62:944–949. [PubMed: 18798269]

Buckley NE, McCoy KL, Mezey E, Bonner T, Zimmer A, Felder CC, Glass M, Zimmer A. Immunomodulation by cannabinoids is absent in mice deficient for the cannabinoid CB(2) receptor. Eur J Pharmacol. 2000; 396:141–149. [PubMed: 10822068]

Buzsáki G, Wang XJ. Mechanisms of gamma oscillations. Annu Rev Neurosci. 2012; 35:203–225. [PubMed: 22443509]

Carta M, Lanore F, Rebola N, Szabo Z, Da Silva SV, Lourenço J, Verraes A, Nadler A, Schultz C, Blanchet C, Mulle C. Membrane lipids tune synaptic transmission by direct modulation of presynaptic potassium channels. Neuron. 2014; 81:787–799. [PubMed: 24486086]

Castillo PE, Younts TJ, Chávez AE, Hashimotodani Y. Endocannabinoid signaling and synaptic function. Neuron. 2012; 76:70–81. [PubMed: 23040807]

Chesler M, Kaila K. Modulation of pH by neuronal activity. Trends Neurosci. 1992; 15:396–402. [PubMed: 1279865]

Chevaleyre V, Castillo PE. Heterosynaptic LTD of hippocampal GABAergic synapses: a novel role of endocannabinoids in regulating excitability. Neuron. 2003; 38:461–472. [PubMed: 12741992]

Chevaleyre V, Castillo PE. Endocannabinoid-mediated metaplasticity in the hippocampus. Neuron. 2004; 43:871–881. [PubMed: 15363397]

Chevaleyre V, Takahashi KA, Castillo PE. Endocannabinoid-mediated synaptic plasticity in the CNS. Annu Rev Neurosci. 2006; 29:37–76. [PubMed: 16776579]

Colgin LL, Denninger T, Fyhn M, Hafting T, Bonnevie T, Jensen O, Moser MB, Moser EI. Frequency of gamma oscillations routes flow of information in the hippocampus. Nature. 2009; 462:353–357. [PubMed: 19924214]

Csicsvari J, Jamieson B, Wise KD, Buzsaáki G. Mechanisms of gamma oscillations in the hippocampus of the behaving rat. Neuron. 2003; 37:311–322. [PubMed: 12546825]

den Boon FS, Chameau P, Schaafsma-Zhao Q, van Aken W, Bari M, Oddi S, Kruse CG, Maccarrone M, Wadman WJ, Werkman TR. Excitability of prefrontal cortical pyramidal neurons is modulated by activation of intracellular type-2 cannabinoid receptors. Proc Natl Acad Sci USA. 2012; 109:3534–3539. [PubMed: 22331871]

Eckert WA 3rd, Willcockson HH, Light AR. Interference of biocytin with opioid-evoked hyperpolarization and membrane properties of rat spinal substantia gelatinosa neurons. Neurosci Lett. 2001; 297:117–120. [PubMed: 11121884]

Galiègue S, Mary S, Marchand J, Dussossoy D, Carrière D, Carayon P, Bouaboula M, Shire D, Le Fur G, Casellas P. Expression of central and peripheral cannabinoid receptors in human immune tissues and leukocyte subpopulations. Eur J Biochem. 1995; 232:54–61. [PubMed: 7556170]

García-Gutiérrez MS, Ortega-Álvaro A, Busquets-García A, Pérez-Ortiz JM, Caltana L, Ricatti MJ, Brusco A, Maldonado R, Manzanares J. Synaptic plasticity alterations associated with memory impairment induced by deletion of CB2 cannabinoid receptors. Neuropharmacology. 2013; 73:388–396. [PubMed: 23796670]

Gerdeman GL, Ronesi J, Lovinger DM. Postsynaptic endocannabinoid release is critical to long-term depression in the striatum. Nat Neurosci. 2002; 5:446–451. [PubMed: 11976704]

Gong JP, Onaivi ES, Ishiguro H, Liu QR, Tagliaferro PA, Brusco A, Uhl GR. Cannabinoid CB2 receptors: immunohistochemical localization in rat brain. Brain Res. 2006; 1071:10–23. [PubMed: 16472786]

Gustafsson B, Wigström H. Hyperpolarization following long-lasting tetanic activation of hippocampal pyramidal cells. Brain Res. 1983; 275:159–163. [PubMed: 6313125]

Hájos N, Freund TF. Distinct cannabinoid sensitive receptors regulate hippocampal excitation and inhibition. Chem Phys Lipids. 2002; 121:73–82. [PubMed: 12505692]

Hashimotodani Y, Ohno-Shosaku T, Maejima T, Fukami K, Kano M. Pharmacological evidence for the involvement of diacylglycerol lipase in depolarization-induced endocanabinoid release. Neuropharmacology. 2008; 54:58–67. [PubMed: 17655882]

Ho BY, Uezono Y, Takada S, Takase I, Izumi F. Coupling of the expressed cannabinoid CB1 and CB2 receptors to phospholipase C and G protein-coupled inwardly rectifying K+ channels. Receptors Channels. 1999; 6:363–374. [PubMed: 10551268]

Jenniches, I., Ternes, S., Albayram, O., Otte, DM., Bach, K., Bindila, L., Michel, K., Lutz, B., Bilkei-Gorzo, A., Zimmer, A. Anxiety, Stress, and Fear Response in Mice with Reduced Endocannabinoid Levels. Biol Psychiatry. 2015. S0006-3223(15)00314-5 Published online April 14, 2015http://dx.doi.org/10.1016/j.biopsych.2015.03.033

Kaczorowski CC, Disterhoft J, Spruston N. Stability and plasticity of intrinsic membrane properties in hippocampal CA1 pyramidal neurons: effects of internal anions. J Physiol. 2007; 578:799–818. [PubMed: 17138601]

Kano M, Ohno-Shosaku T, Hashimotodani Y, Uchigashima M, Watanabe M. Endocannabinoid-mediated control of synaptic transmission. Physiol Rev. 2009; 89:309–380. [PubMed: 19126760]

Katona I, Freund TF. Multiple functions of endocannabinoid signaling in the brain. Annu Rev Neurosci. 2012; 35:529–558. [PubMed: 22524785]

Katona I, Sperlágh B, Sík A, Käfalvi A, Vizi ES, Mackie K, Freund TF. Presynaptically located CB1 cannabinoid receptors regulate GABA release from axon terminals of specific hippocampal interneurons. J Neurosci. 1999; 19:4544–4558. [PubMed: 10341254]

Kim J, Alger BE. Reduction in endocannabinoid tone is a homeostatic mechanism for specific inhibitory synapses. Nat Neurosci. 2010; 13:592–600. [PubMed: 20348918]

Kim J, Li Y. Chronic activation of CB2 cannabinoid receptors in the hippocampus increases excitatory synaptic transmission. J Physiol. 2015; 593:871–886. [PubMed: 25504573]

Kowalski, J., Gan, J., Jonas, P., Pernía-Andrade, AJ. Intrinsic membrane properties determine hippocampal differential firing pattern in vivo in anesthetized rats. Hippocampus. 2015. Published online November 25, 2015http://dx.doi.org/10.1002/hipo.22550

Kreitzer AC, Carter AG, Regehr WG. Inhibition of interneuron firing extends the spread of endocannabinoid signaling in the cerebellum. Neuron. 2002; 34:787–796. [PubMed: 12062024]

Le Duigou C, Simonnet J, Teleñczuk MT, Fricker D, Miles R. Recurrent synapses and circuits in the CA3 region of the hippocampus: an associative network. Front Cell Neurosci. 2014; 7:262. [PubMed: 24409118]

Lee D, Lin BJ, Lee AK. Hippocampal place fields emerge upon single-cell manipulation of excitability during behavior. Science. 2012; 337:849–853. [PubMed: 22904011]

Li Y, Kim J. Neuronal expression of CB2 cannabinoid receptor mRNAs in the mouse hippocampus. Neuroscience. 2015; 311:253–267. [PubMed: 26515747]

Li Y, Kim J. Deletion of CB2 cannabinoid receptors reduces synaptic transmission and long-term potentiation in the mouse hippocampus. Hippocampus. 2016; 26:275–281. [PubMed: 26663094]

Li X, Rubio FJ, Zeric T, Bossert JM, Kambhampati S, Cates HM, Kennedy PJ, Liu QR, Cimbro R, Hope BT, et al. Incubation of methamphetamine craving is associated with selective increases in expression of Bdnf and trkb, glutamate receptors, and epigenetic enzymes in cue-activated fos-expressing dorsal striatal neurons. J Neurosci. 2015; 35:8232–8244. [PubMed: 26019338]

Liu QR, Pan CH, Hishimoto A, Li CY, Xi ZX, Llorente-Berzal A, Viveros MP, Ishiguro H, Arinami T, Onaivi ES, Uhl GR. Species differences in cannabinoid receptor 2 (CNR2 gene): identification of novel human and rodent CB2 isoforms, differential tissue expression and regulation by cannabinoid receptor ligands. Genes Brain Behav. 2009; 8:519–530. [PubMed: 19496827]

Liu QR, Rubio FJ, Bossert JM, Marchant NJ, Fanous S, Hou X, Shaham Y, Hope BT. Detection of molecular alterations in methamphetamine-activated Fos-expressing neurons from a single rat dorsal striatum using fluorescence-activated cell sorting (FACS). J Neurochem. 2014; 128:173–185. [PubMed: 23895375]

Lodge D, Tidball P, Mercier MS, Lucas SJ, Hanna L, Ceolin L, Kritikos M, Fitzjohn SM, Sherwood JL, Bannister N, et al. Antagonists reversibly reverse chemical LTD induced by group I, group II and group III metabotropic glutamate receptors. Neuropharmacology. 2013; 74:135–146. [PubMed: 23542080]

Mackie K, Lai Y, Westenbroek R, Mitchell R. Cannabinoids activate an inwardly rectifying potassium conductance and inhibit Q-type calcium currents in AtT20 cells transfected with rat brain cannabinoid receptor. J Neurosci. 1995; 15:6552–6561. [PubMed: 7472417]

Maier N, Tejero-Cantero A, Dorrn AL, Winterer J, Beed PS, Morris G, Kempter R, Poulet JFA, Leibold C, Schmitz D. Coherent phasic excitation during hippocampal ripples. Neuron. 2011; 72:137–152. [PubMed: 21982375]

Maier N, Morris G, Schuchmann S, Korotkova T, Ponomarenko A, Böhm C, Wozny C, Schmitz D. Cannabinoids disrupt hippocampal sharp wave-ripples via inhibition of glutamate release. Hippocampus. 2012; 22:1350–1362. [PubMed: 21853502]

Majumdar D, Maunsbach AB, Shacka JJ, Williams JB, Berger UV, Schultz KP, Harkins LE, Boron WF, Roth KA, Bevensee MO. Localization of electrogenic Na/bicarbonate cotransporter NBCe1 variants in rat brain. Neuroscience. 2008; 155:818–832. [PubMed: 18582537]

Marchalant Y, Brownjohn PW, Bonnet A, Kleffmann T, Ashton JC. Validating antibodies to the cannabinoid CB2 receptor: Antibody sensitivity is not evidence of antibody specificity. J Histochem Cytochem. 2014; 62:395–404. [PubMed: 24670796]

Marinelli S, Pacioni S, Cannich A, Marsicano G, Bacci A. Self-modulation of neocortical pyramidal neurons by endocannabinoids. Nat Neurosci. 2009; 12:1488–1490. [PubMed: 19915567]

Marsicano G, Goodenough S, Monory K, Hermann H, Eder M, Cannich A, Azad SC, Cascio MG, Gutiérrez SO, van der Stelt M, et al. CB1 cannabinoid receptors and on-demand defense against excitotoxicity. Science. 2003; 302:84–88. [PubMed: 14526074]

Monory K, Massa F, Egertová M, Eder M, Blaudzun H, Westenbroek R, Kelsch W, Jacob W, Marsch R, Ekker M, et al. The endocannabinoid system controls key epileptogenic circuits in the hippocampus. Neuron. 2006; 51:455–466. [PubMed: 16908411]

Morgan NH, Stanford IM, Woodhall GL. Functional CB2 type cannabinoid receptors at CNS synapses. Neuropharmacology. 2009; 57:356–368. [PubMed: 19616018]

Munro S, Thomas KL, Abu-Shaar M. Molecular characterization of a peripheral receptor for cannabinoids. Nature. 1993; 365:61–65. [PubMed: 7689702]

Onaivi ES. Neuropsychobiological evidence for the functional presence and expression of cannabinoid CB2 receptors in the brain. Neuropsychobiology. 2006; 54:231–246. [PubMed: 17356307]

Onaivi ES. Commentary: Functional neuronal CB2 cannabinoid receptors in the CNS. Curr Neuropharmacol. 2011; 9:205–208. [PubMed: 21886591]

Palmer MJ, Irving AJ, Seabrook GR, Jane DE, Collingridge GL. The group I mGlu receptor agonist DHPG induces a novel form of LTD in the CA1 region of the hippocampus. Neuropharmacology. 1997; 36:1517–1532. [PubMed: 9517422]

Robbe D, Kopf M, Remaury A, Bockaert J, Manzoni OJ. Endogenous cannabinoids mediate long-term synaptic depression in the nucleus accumbens. Proc Natl Acad Sci USA. 2002; 99:8384–8388. [PubMed: 12060781]

Robbe D, Montgomery SM, Thome A, Rueda-Orozco PE, McNaughton BL, Buzsaki G. Cannabinoids reveal importance of spike timing coordination in hippocampal function. Nat Neurosci. 2006; 9:1526–1533. [PubMed: 17115043]

Ruffin VA, Salameh AI, Boron WF, Parker MD. Intracellular pH regulation by acid-base transporters in mammalian neurons. Front Physiol. 2014; 5:43. [PubMed: 24592239]

Salter MW, Beggs S. Sublime microglia: expanding roles for the guardians of the CNS. Cell. 2014; 158:15–24. [PubMed: 24995975]

Schmöle AC, Lundt R, Gennequin B, Schrage H, Beins E, Krämer A, Zimmer T, Limmer A, Zimmer A, Otte DM. Expression Analysis of CB2-GFP BAC Transgenic Mice. PLoS ONE. 2015; 10:e0138986. [PubMed: 26406232]

Schomburg EW, Fernández-Ruiz A, Mizuseki K, Berényi A, Anastassiou CA, Koch C, Buzsáki G. Theta phase segregation of input-specific gamma patterns in entorhinal-hippocampal networks. Neuron. 2014; 84:470–485. [PubMed: 25263753]

Sloviter RS. Permanently altered hippocampal structure, excitability, and inhibition after experimental status epilepticus in the rat: the “dormant basket cell” hypothesis and its possible relevance to temporal lobe epilepsy. Hippocampus. 1991; 1:41–66. [PubMed: 1688284]

Stella N, Schweitzer P, Piomelli D. A second endogenous cannabinoid that modulates long-term potentiation. Nature. 1997; 388:773–778. [PubMed: 9285589]

Sugiura T, Kobayashi Y, Oka S, Waku K. Biosynthesis and degradation of anandamide and 2-arachidonoylglycerol and their possible physiological significance. Prostaglandins Leukot Essent Fatty Acids. 2002; 66:173–192. [PubMed: 12052034]

Takahashi KA, Castillo PE. The CB1 cannabinoid receptor mediates glutamatergic synaptic suppression in the hippocampus. Neuroscience. 2006; 139:795–802. [PubMed: 16527424]

Tropp Sneider J, Chrobak JJ, Quirk MC, Oler JA, Markus EJ. Differential behavioral state-dependence in the burst properties of CA3 and CA1 neurons. Neuroscience. 2006; 141:1665–1677. [PubMed: 16843607]

Van Sickle MD, Duncan M, Kingsley PJ, Mouihate A, Urbani P, Mackie K, Stella N, Makriyannis A, Piomelli D, Davison JS, et al. Identification and functional characterization of brainstem cannabinoid CB2 receptors. Science. 2005; 310:329–332. [PubMed: 16224028]

Wilson RI, Nicoll RA. Endogenous cannabinoids mediate retrograde signalling at hippocampal synapses. Nature. 2001; 410:588–592. [PubMed: 11279497]

Wilson RI, Nicoll RA. Endocannabinoid signaling in the brain. Science. 2002; 296:678–682. [PubMed: 11976437]

Wittner L, Miles R. Factors defining a pacemaker region for synchrony in the hippocampus. J Physiol. 2007; 584:867–883. [PubMed: 17823211]

Wulff P, Ponomarenko AA, Bartos M, Korotkova TM, Fuchs EC, Bähner F, Both M, Tort ABL, Kopell NJ, Wisden W, Monyer H. Hippocampal theta rhythm and its coupling with gamma oscillations require fast inhibition onto parvalbumin-positive interneurons. Proc Natl Acad Sci USA. 2009; 106:3561–3566. [PubMed: 19204281]

Xi ZX, Peng XQ, Li X, Song R, Zhang HY, Liu QR, Yang HJ, Bi GH, Li J, Gardner EL. Brain cannabinoid CB_2 receptors modulate cocaine's actions in mice. Nat Neurosci. 2011; 14:1160–1166. [PubMed: 21785434]

Young SR, Chuang SC, Zhao W, Wong RKS, Bianchi R. Persistent receptor activity underlies group I mGluR-mediated cellular plasticity in CA3 neuron. J Neurosci. 2013; 33:2526–2540. [PubMed: 23392681]

Younts TJ, Chevaleyre V, Castillo PE. CA1 pyramidal cell theta-burst firing triggers endocannabinoid-mediated long-term depression at both somatic and dendritic inhibitory synapses. J Neurosci. 2013; 33:13743–13757. [PubMed: 23966696]

Zhang HY, Gao M, Liu QR, Bi GH, Li X, Yang HJ, Gardner EL, Wu J, Xi ZX. Cannabinoid CB2 receptors modulate midbrain dopamine neuronal activity and dopamine-related behavior in mice. Proc Natl Acad Sci USA. 2014; 111:E5007–E5015. [PubMed: 25368177]

Zimmer A, Zimmer AM, Hohmann AG, Herkenham M, Bonner TI. Increased mortality, hypoactivity, and hypoalgesia in cannabinoid CB1 receptor knockout mice. Proc Natl Acad Sci USA. 1999; 96:5780–5785. [PubMed: 10318961]

Highlights

- CB_2Rs are expressed in hippocampal principal neurons
- CB_2Rs mediate a cell type-specific self-inhibitory plasticity in CA3/CA2 PCs
- CB_2Rs reduce the spike probability of CA3 PCs and alter gamma oscillations in vivo
- CB_2Rs act complementary to presynaptic CB_1Rs

In Brief

The neuronal expression of CB_2Rs has been a matter of long-standing debate. Stempel et al. demonstrate that CB_2Rs are expressed in hippocampal principal cells and modulate neuronal function both in vitro and in vivo.

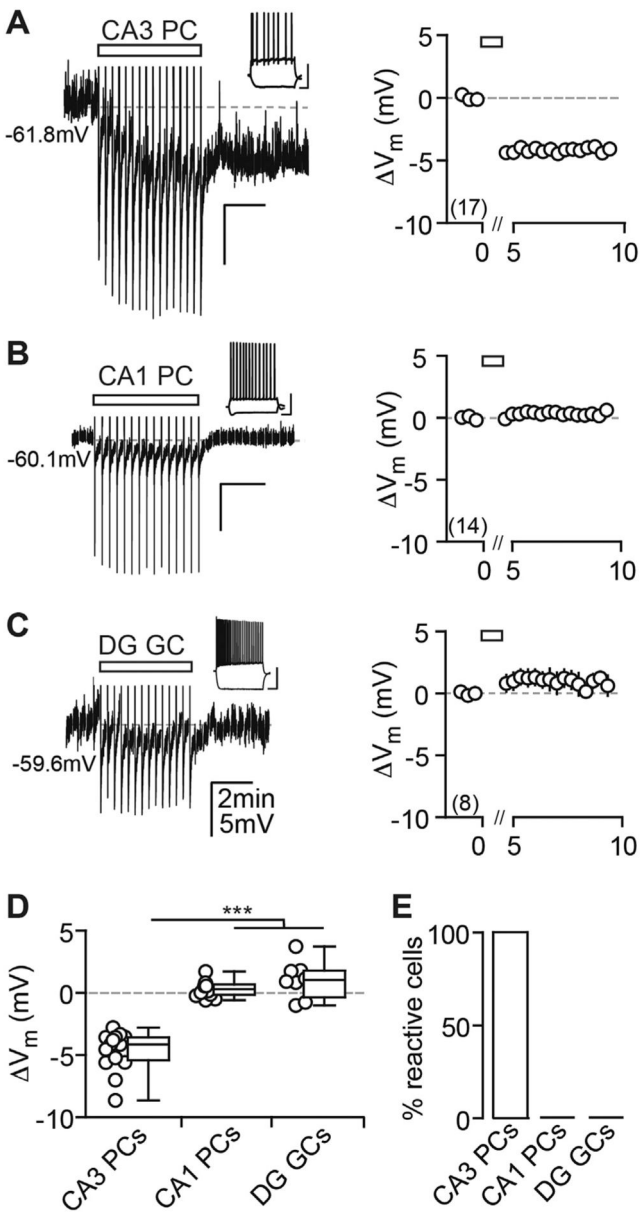

Figure 1. AP Firing Induces a Cell Type-Specific V_m Hyperpolarization in Hippocampal Principal Cells

(A–C) Current injection-triggered AP trains (rectangle) induce a long-lasting V_m hyperpolarization in CA3 PCs (A), but not in CA1 PCs (B) and DG GCs (C). Left: exemplary pp recordings of each principal cell population are shown. APs have been truncated and test pulses cut for display purposes in this and all later figures. Insets: firing patterns are shown (scale bar, 40 mV, 0.2 s). Right: summary time course shows the ΔV_m average for CA3 PCs: n(N) = 17(13), CA1 PCs: n(N) = 14(4), and DG GCs: n(N) = 8(4). The x axis is discontinued for the duration of the AP train.

(D) The ΔV_m of each recorded cell (circles) and the median and 25th and 75th percentiles of the average ΔV_m calculated from the first minute after the last AP train are shown for CA3 PCs (−4.1, −5.4, and −3.6 mV), CA1 PCs (0.30, −0.15 to 0.68 mV) and DG GCs (1.04,

−0.35 to 1.8 mV). Kruskal-Wallis with Dunn's post-test, $p < 0.05$ for CA3 PCs versus CA1 PCs and DG GCs.

(E) Percentage (%) of reactive cells is shown.

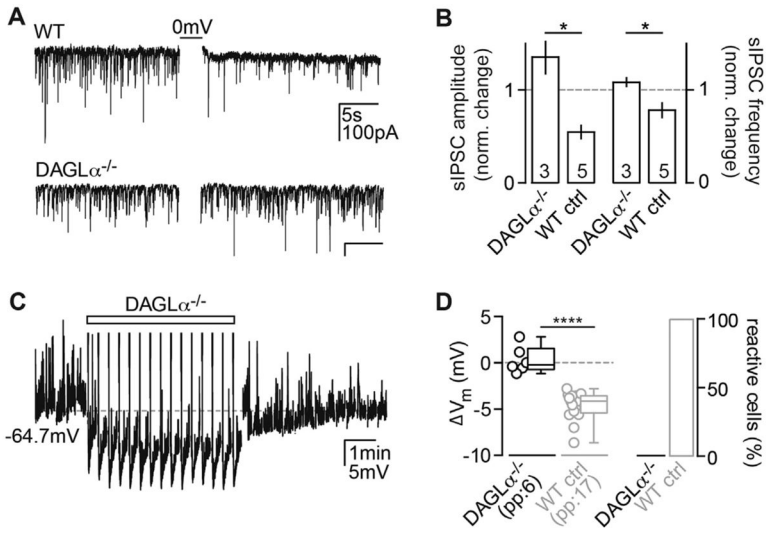

Figure 2. The eCB 2-AG Mediates the Hyperpolarization

(A) As a control, sIPSCs were recorded from WT and DAGLα$^{-/-}$ CA3 PCs to test for the presence of DSI. In contrast to a DSI+ WT CA3 PC (upper trace), depolarization of a DAGLα$^{-/-}$ CA3 PC (0 mV for 3 × 1 s) failed to induce DSI (lower trace).

(B) The normalized change in amplitude (left) and frequency (right) of sIPSCs in DAGLα$^{-/-}$ CA3 PCs (n(N) = 3(1): 1.4 ± 0.17 and 1.2 ± 0.05) differed significantly from WT controls (n(N) = 5(1)), 0.55 ± 0.1 and 0.78 ± 0.1, Mann-Whitney test, p = 0.036). The absolute sIPSC amplitude and frequency after DSI induction in the DAGLα KO do not differ from baseline (Wilcoxon test, p = 0.25).

(C) Example V_m response of a DAGLα$^{-/-}$ CA3 PC to the AP stimulus (rectangle) is shown.

(D) Left: the ΔV_m of each recorded cell (circles) and the median and 25th and 75th percentiles of the average ΔV_m are shown for n(N) = 6(3) experiments in pp (−0.2, −0.7, and 1.5 mV; Wilcoxon test, p = 0.84 in comparison to baseline). Right: Percentage of reactive cells is shown. For statistical comparison, the V_m values from WT CA3 PCs (Figure 1) are re-plotted in gray (Mann Whitney test, p < 0.0001).

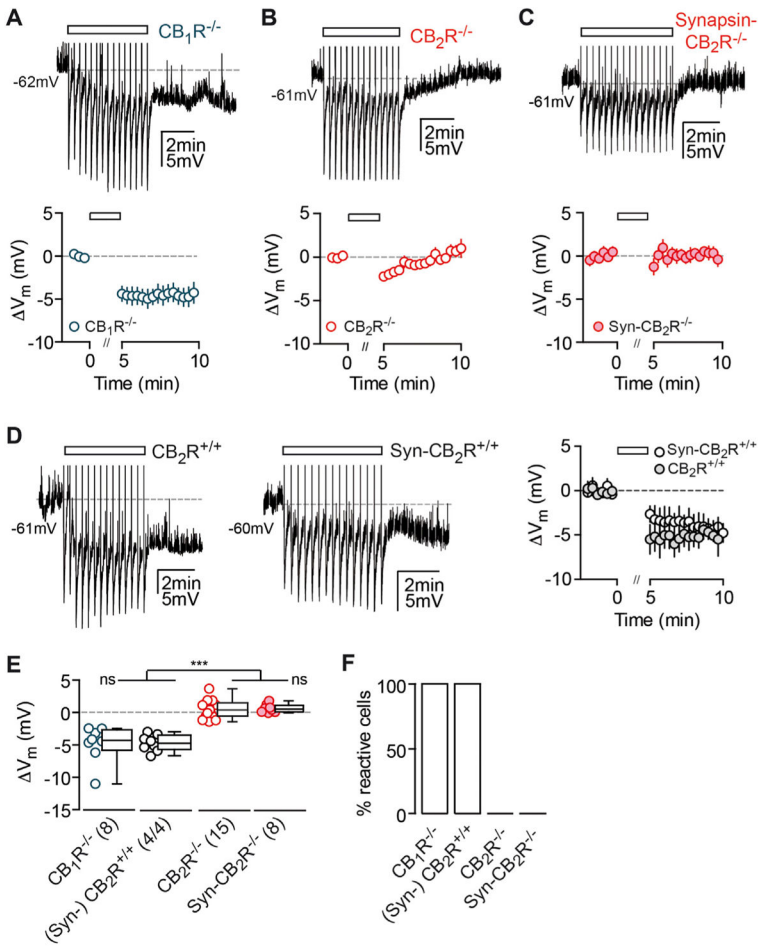

Figure 3. The Long-Lasting Hyperpolarization Is Absent in CB_2R-Deficient Mice

(A–C) AP trains (rectangle) induce a long-lasting hyperpolarization in $CB_1R^{-/-}$ CA3 PCs (A), but not in CA3 PCs of $CB_2R^{-/-}$ (B) and Syn-$CB_2R^{-/-}$ mice (C). Left: exemplary pp recordings of KO CA3 PCs are shown. Right: summary time course shows the average ΔV_m of CA3 PCs recorded from $CB_1R^{-/-}$: n(N) = 8(6), $CB_2R^{-/-}$: n(N) = 15(7), and Syn-$CB_2R^{-/-}$: n(N) = 8(5). The x axis is discontinued for the duration of the AP train.

(D) Same is shown as for (A)–(C) except for WT littermate controls of $CB_2R^{-/-}$ and Syn-$CB_2R^{-/-}$ mice: n(N) = 4(3)/4(2).

(E) The ΔV_m of each recorded cell (circles) and the median and 25th and 75th percentiles of the average ΔV_m (min 9–10) are shown for CA3 PCs recorded in $CB_1R^{-/-}$ (−4.3, −5.8, and −2.6 mV), (Syn-)$CB_2R^{+/+}$ littermates (−4.7, −5.8 to −3.5 mV), $CB_2R^{-/-}$ (0.39, −0.57 to 1.4 mV), and Syn- $CB_2R^{-/-}$ (0.53, 0.086 to 1.1 mV). Kruskal-Wallis with Dunn's post test, $p < 0.0001$ for [WT and $CB_1R^{-/-}$] versus [$CB_2R^{-/-}$ and Syn-$CB_2R^{-/-}$]. The average ΔV_m of WT versus $CB_1R^{-/-}$ and $CB_2R^{-/-}$ versus Syn-$CB_2R^{-/-}$ did not differ significantly.

(F) Percentage of reactive cells are shown.

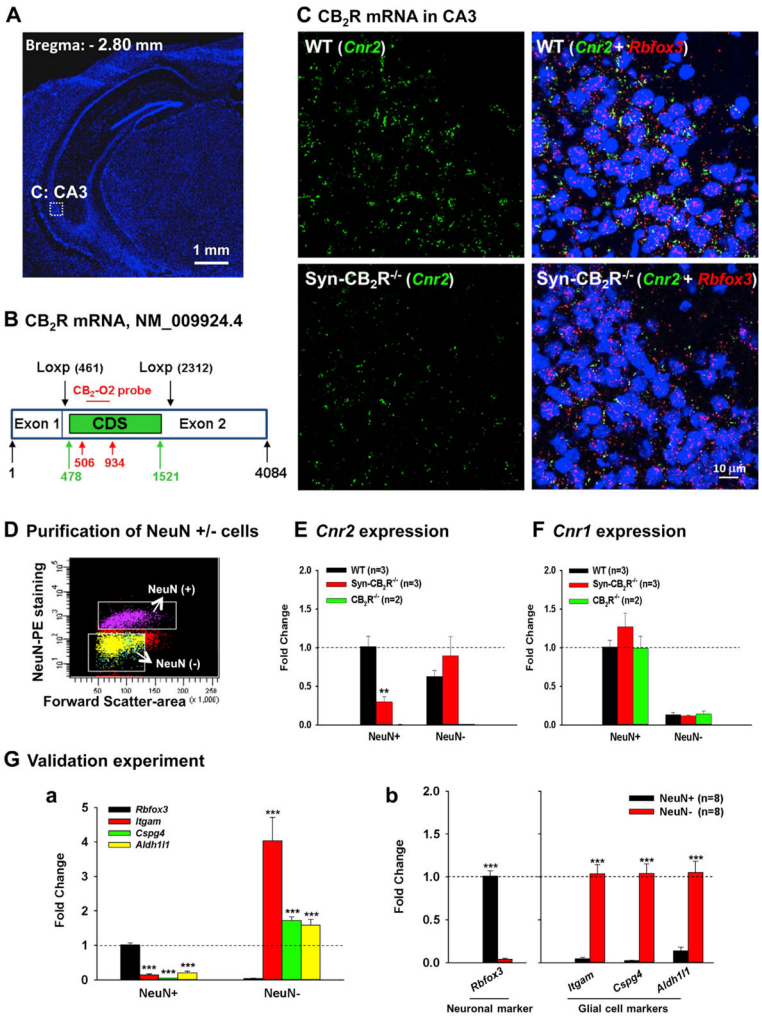

Figure 4. Neuronal CB_2R mRNA Expression in the Hippocampus by RNAscope ISH and FACS-qPCR Assays

(A) Hippocampal image (DAPI staining) illustrates the target region (CA3) in (C).

(B) The CB_2R mRNA structure in CB_2R-floxed mice and the target gene region of a CB_2R RNAscope probe (CB_2-O2, 506–934 bp) used to detect CB_2R mRNA. The CB_2-O2 probe targets the floxed region of mouse CB_2R mRNA (NM_009924.4) in CB_2R-floxed mice. CDS, (CB_2R)-coding DNA sequence (478–1,521 bp).

(C) CB_2R mRNA staining illustrates significant CB_2R (*Cnr2*, green) and NeuN (*Rbfox,* red) mRNA co-localization in WT hippocampal CA3 neurons (upper panels), while such co-localization is substantially diminished in Syn-$CB_2R^{-/-}$ (lower panels).

(D) A representative image shows FACS-sorted NeuN+ neurons and NeuN− non-neuronal cells in the hippocampus.

(E) The qPCR assays show that CB_2R mRNA is detected mainly in NeuN+ hippocampal cells of WT mice, while the CB_2R mRNA in NeuN+ hippocampal cells in Syn-$CB_2R^{-/-}$ mice was substantially reduced (~70% reduction), and abolished in the $CB_2R^{-/-}$ mice.

(F) The qPCR assays for CB_1R mRNA (as controls) in the same samples demonstrate similar levels of CB_1R mRNA expression in NeuN+ neurons and NeuN− cells in WT, Syn-$CB_2R^{-/-}$, and const. $CB_2R^{-/-}$ mice.

(G) The qPCR assay results of neuronal and glial markers in two cell populations to examine the purity of sorted cells, illustrating that *Rbfox3* was detected mainly in FACS-sorted NeuN + neurons (a), but not in NeuN− cells (b). In contrast, the glial marker genes *Itgam*, *Cspg4*, and *Aldh1l1* were mainly detected in NeuN− nonneuronal cells (b), but not in NeuN+ hippocampal neurons (a). Data shown in (a) were normalized to *Rbfox3* expression in the NeuN+ population, which was defined as 1. Data shown in (b) were normalized to each respective marker gene level in NeuN+ (*Rbfox3*) and NeuN− cells (all three glial markers).

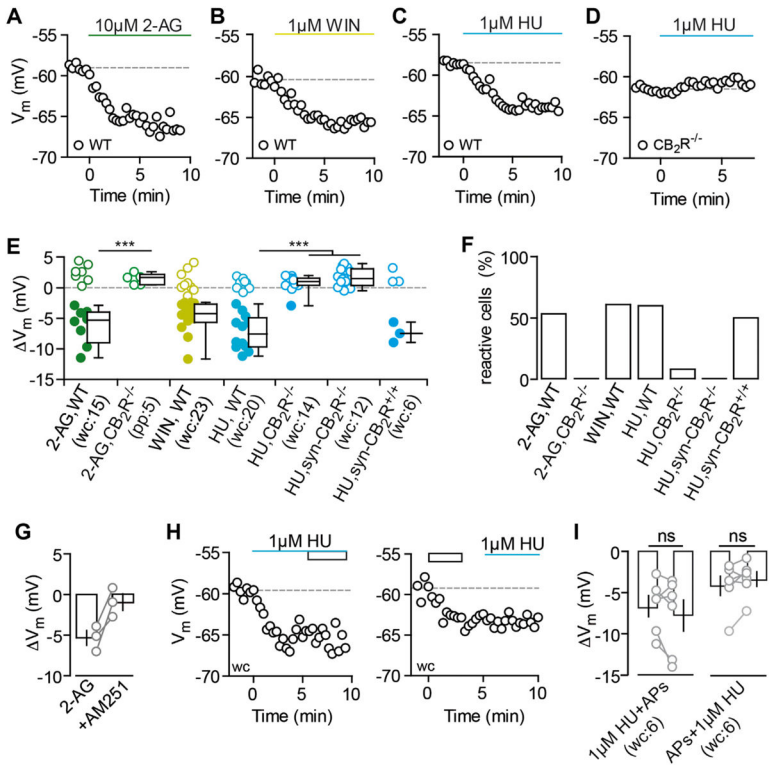

Figure 5. CB_2R Agonists Mimic and Occlude the AP-Driven Hyperpolarization

(A–D) Exemplary V_m time courses of wc CA3 PC recordings are shown for the application of 10 µM2-AG (A), 1 µM WIN (B), and 1 µM HU (C) that hyperpolarize CA3 PCs. The hyperpolarizing effect of HU is gone in the $CB_2R^{-/-}$ (D).

(E and F) The ΔV_m of each recorded cell (circles) and the median and 25th and 75th percentiles of the average ΔV_m (E) as well as the percentage of reactive cells (F) are shown for the application of 2-AG in WT (wc, n(N) = 15(5): −5.3, −9.0 to −3.9 mV; 53.3%) and in $CB_2R^{-/-}$ (pp, n(N) = 5(2): 1.6, 0.5 to 2.2 mV; 0%), WIN in WT (wc, n(N) = 23(15): −4.2, −5.6 to −2.7 mV; 60.9%), HU in WT (wc, n(N) = 20(10): −7.6, −9.7 to −4.9 mV; 60%), HU in $CB_2R^{-/-}$ (wc, n(N) = 12(3): 0.9, 0.3 to 1.5 mV; 8.3%), HU in Syn-$CB_2R^{-/-}$ (wc, n(N) = 14(5): 1.4, 0.3 to 3 mV, 0%), and HU in Syn-$CB_2R^{+/+}$ (wc, n(N) = 6(4): −7.5, −9 to −5.7 mV; 50%). Note that the filled circles indicate reactive cells. Green, 2-AG; yellow, WIN; blue, HU. Kruskal-Wallis with Dunn's post-test, $p < 0.05$ for 2-AG and HU in $CB_2R^{-/-}$ versus WT.

(G) AM-251 reverses the hyperpolarization induced by 2-AG in n(N) = 3(3) CA3 PCs (−5.3 ± 0.9 mV and −0.9 ± 1 mV, respectively).

(H) The HU-induced hyperpolarization (blue line) occludes further hyperpolarization of CA3 PCs in response to APs (rectangle) and vice versa. Exemplary ΔV_m time courses of CA3 PCs that hyperpolarize in response to HU (left) and AP trains (right) are shown.

(I) Single-occlusion experiments (gray circles) and mean ± SEM (black) are shown for each condition. Average ΔV_m for HU followed by APs (left, n(N) = 6(4): −6.6 ± 1.3 and −7.8 ± 1.9 mV; paired t test, $p = 0.24$) and APs followed by HU (right, n(N) = 6(6): −4.2 ± 1.2 and −3.4 ± 0.9 mV, $p = 0.19$).

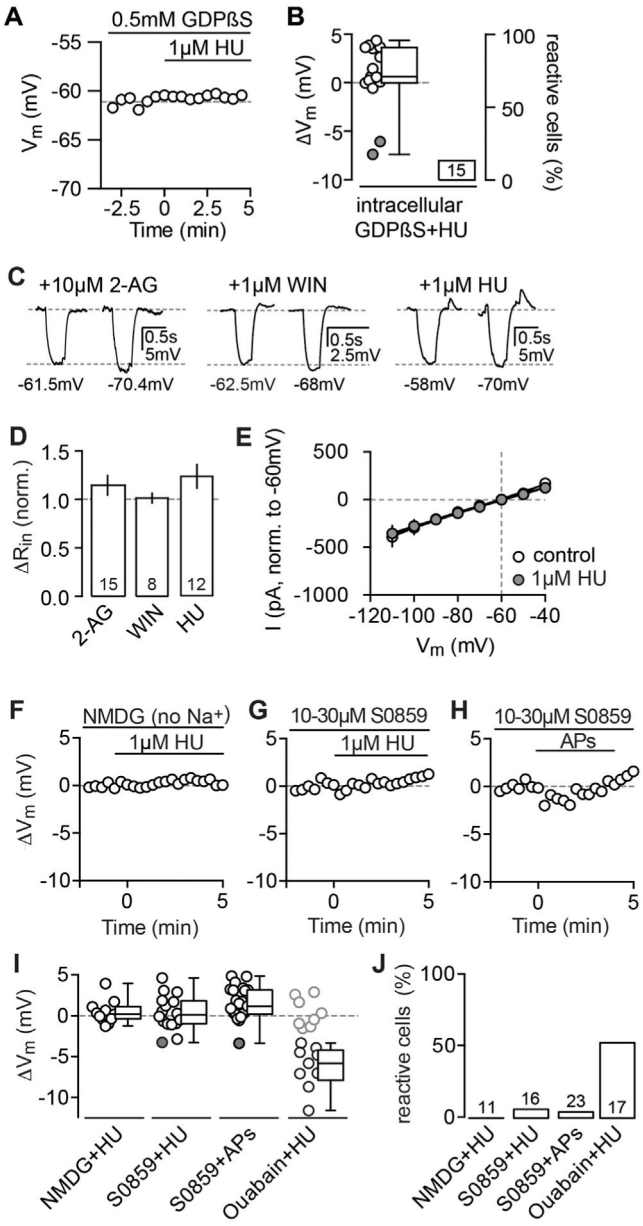

Figure 6. The Hyperpolarization Is Mediated by a G Protein- and Na^+-Dependent Modulation of the NBC

(A) Exemplary ΔV_m time courses of wc CA3 PC recordings with internal application of 0.5 mM GDPβS. The subsequent application of 1 µM HU fails to hyperpolarize the CA3 PC.

(B) The ΔV_m of each recorded cell (circles) and the median and 25th and 75th percentiles of the average ΔV_m (left) as well as the percentage of reactive cells (right) are shown for GDPβS+HU (n(N) = 15(5): 0.6, −0.04 and 3.6 mV; 13.3%) and are significantly different from control WT cells (ΔV_m: $p < 0.0001$, compare to Figure 5E). Note that the remaining reactive cells (indicted by filled circles) are most likely caused by an insufficient diffusion of GDPβS given the short incubation of 5 min to prevent washout.

(C) Exemplary V_m traces of reactive CA3 PCs recorded in wc configuration that hyperpolarized in response to 10 µM 2-AG (left), 1 µM WIN (middle), and 1 µM HU (right).

The R_{in} was calculated from the steady-state response to a −80-pA test pulse. In each panel, the left trace represents the control condition (1 min before agonist application) and the right trace is taken from 5 to 10 min after the drug was bath applied. The respective V_m values are indicated below each trace.

(D) Summary bar graph of all reactive cells shows the normalized ΔR_{in} (mean ± SEM) after drug application for 2-AG (n = 8: 1.1 ± 0.1), WIN (n = 14: 1.01 ± 0.05), and HU (n = 12: 1.2 ± 0.1) that does not differ significantly from baseline levels (paired t test for 2-AG, WIN, and HU: p = 0.30, 0.99, and 0.12).

(E) IV plot of n(N) = 4(2) reactive CA3 PCs that were recorded at different holding potentials in voltage clamp (−110 to 40 mV, 10-mV steps) before and after the application of HU. The hyperpolarization was not accompanied by a change in the IV relationship (normalized to −60 mV, paired t test: p = 0.66).

(F–H) Replacement of Na^+ with NMDG in the ACSF as well as block of the NBC by preincubation of the antagonist S0859 abolished the hyperpolarization. Examples of ΔV_m values for the application of HU in NMDG (F), HU in S0859 (G), and AP stimulation in S0859 in CA3 PCs (H) are shown.

(I) The ΔV_m of each recorded cell (circles) and the median and 25^{th} and 75^{th} percentiles of the average ΔV_m (left) as well as the percentage of reactive cells (right) are shown for the application of HU in NMDG (wc, n(N) = 11(5): 1.9, −1.1 to 2.8 mV; 0%), HU in S0859 (wc, n(N) = 16(6): 0.01, −1.1 to 1.7 mV, 6.25%), APs in S0859 (wc, n(N) = 23(9): 1.1, 0.1 to 3 mV, 4.3%), and, as a control, HU in 10 μM ouabain (wc, n(N) = 17(6), −5.8, −7.9 to −4.2 mV, 52.9%).

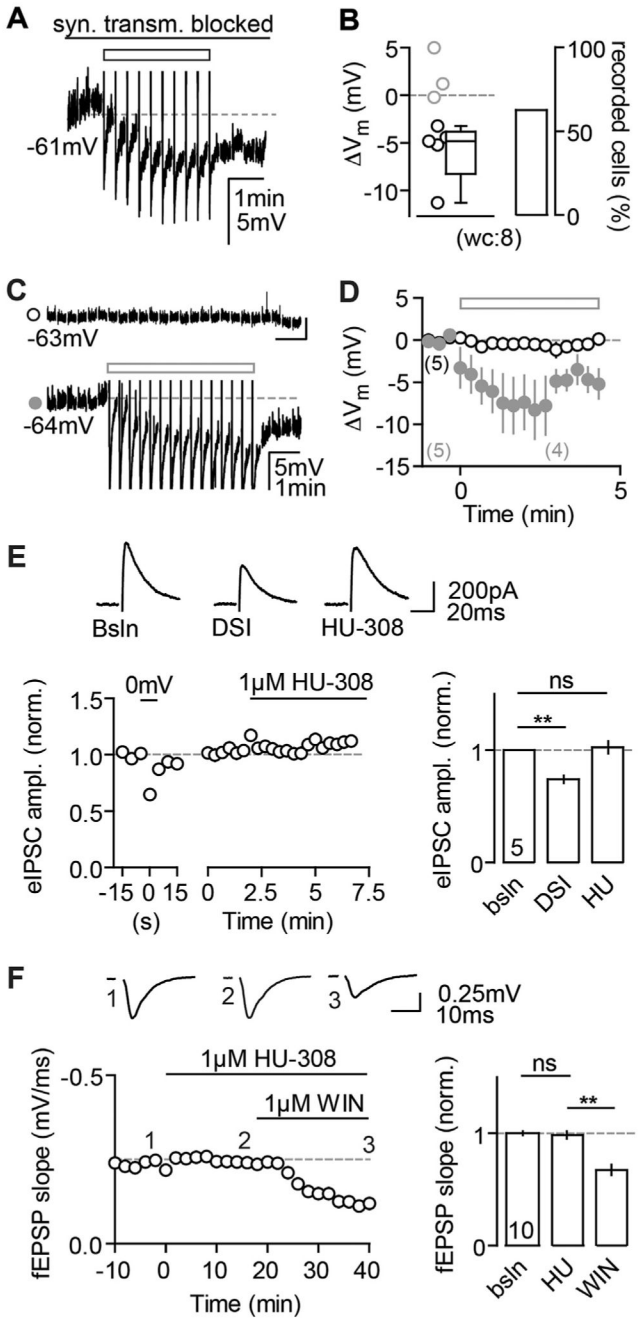

Figure 7. Comparison of CB_2R- versus Presynaptic CBR-Mediated Effects

(A and B) The continuous block of glutamatergic (20 μM NBQX, 50 μM D-AP5) as well as GABAergic (1 μM Gabazine, 1 μM CGP) transmission does not abolish the AP-induced hyperpolarization. (A) Example wc recording of a reactive CA3 PC in response to the AP train (rectangle) is shown. (B) The ΔV_m of each recorded cell (circles) and the median and 25^{th} and 75^{th} percentiles of the average ΔV_m of all reactive cells are shown for n(N) = 8(2) experiments (−4.8, −8.3, and −3.8 mV; left). The percentage of reactive cells is 62.5% (right).

(C) Dual pp recording of 2 CA3 PCs. AP firing in a control cell (lower trace) elicits a hyperpolarization in this, but not in the other cell (upper trace). The AHPs of the control cell are clipped for display purposes.
(D) In 5/5 recordings (N = 5), the control cell hyperpolarized in response to the AP trains (filled gray circles, ΔV_m: −6.0 ± 1.5 mV), whereas the unstimulated cell did not (open black circles, ΔV_m: 0.02 ± 0.6 mV).
(E and F) CB_2R agonists cannot mimic CB_1R-mediated depression of synaptic transmission. (E) HU has no effect on DSI-positive eIPSCs. Left: example of a CA3 PC recorded in wc configuration is shown. Depolarization of the neuron results in a transient reduction of eIPSC amplitude, whereas bath application of HU does not. Right: mean normalized eIPSC amplitudes of n(N) = 5(4) experiments for DSI (0.7 ± 0.03) and HU application (1 ± 0.05) in comparison to baseline (paired t test, p = 0.0016 and p = 0.67) are shown. (F) WIN, but not HU, suppresses evoked field responses in CA3. Left: exemplary fEPSP recording with HU and WIN bath application is shown. Right: mean normalized fEPSP slopes for HU (1 ± 0.03) and WIN (0.7 ± 0.05) in comparison to baseline (paired t test, p = 0.33 and p < 0.001) are shown.

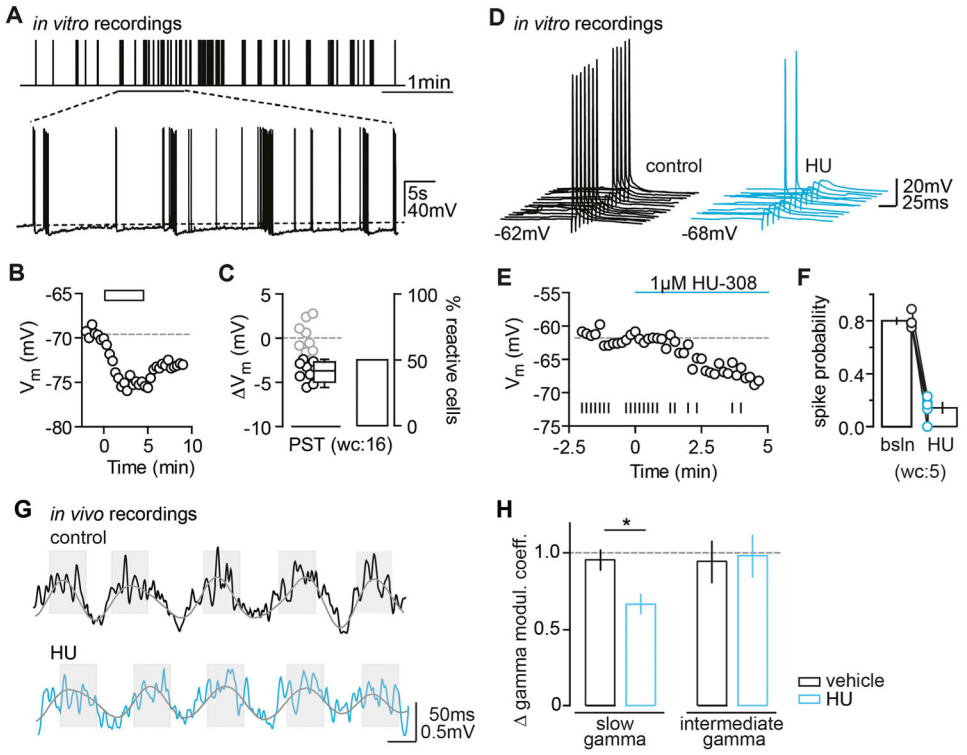

Figure 8. Functional Relevance of CB_2R Activation Probed In Vitro and In Vivo

(A–C) PSTs trigger long-lasting hyperpolarization. (A) Schematic shows the presented PST (upper panel) as well as a segment of an exemplary V_m trace of a rat CA3 PC that fires in response to the respective stimulus (lower panel). (B) V_m time plot shows the same CA3 PC responding to the PST (rectangle) with a long-lasting hyperpolarization. (C) Left: the ΔV_m of each recorded cell (circles) and the median and 25th and 75th percentiles of the average ΔV_m of reactive rat CA3 PCs (wc, n(N) = 16(6): −4.5, −6.7, and −2.7 mV) are shown. Right: percentage of reactive cells (50%) is shown.

(D–F) CB_2R activation reduces the spike probability of CA3 PCs. (D) The spike probability of a CA3 PC in response to the application of the CB_2R agonist HU is shown. Example traces show spikes elicited by synaptic stimulation during control conditions (black) and 5 min after HU application (red). The baseline and hyperpolarized V_m values are indicated below the traces. (E) Time plot of the V_m (circles) show the same cell and its AP firing (vertical lines) for each given V_m. (F) Summary graph shows the spike probability for n(N) = 5(3) reactive cells under baseline and agonist conditions (0.8 ± 0.02 and 0.14 ± 0.04, respectively). The change in spike probability was accompanied by an average V_m hyperpolarization of −6.3 ± 0.3 mV.

(G and H) CB_2Rs regulate hippocampal gamma oscillations in vivo: altered coupling of gamma and theta oscillations after HU application. (G) LFP signal traces (1–150 Hz band-pass filtered) were recorded in the CA3 area during exploratory behavior before (upper panel) and 30 min after (lower panel) the i.p. administration of HU (10 mg/kg). Note that the typical association of high-amplitude gamma oscillations with theta oscillation peaks (shades) and low-amplitude gamma oscillations with theta oscillation troughs is altered after the CB_2R agonist administration. (H) The theta modulation of slow (30–85 Hz), but not

intermediate (65–120 Hz), gamma oscillations was reduced by the agonist administration (vehicle: n(N) = 15(10), agonist: n(N) = 13(10), $F_{1,13} = 9.1$, $p = 0.010$, slow, $F_{1,13} = 0.0$, $p = 0.86$, ANOVA).